HHS Public Access

Author manuscript

Int J Intell Robot Appl. Author manuscript; available in PMC 2018 February 01.

Published in final edited form as:

Int J Intell Robot Appl. 2017 February ; 1(1): 6–18. doi:10.1007/s41315-016-0003-5.

Bilateral Control of Functional Electrical Stimulation and Robotics-based Telerehabilitation

Mr. Naji Alibeji,
Department of Mechanical Engineering and Materials Science, University of Pittsburgh, Pittsburgh, PA,USA 15261

Dr. Brad E. Dicianno, MD, and
Department of Physical Medicine and Rehabilitation, University of Pittsburgh, Pittsburgh, PA,USA 15261

Dr. Nitin Sharma, PhD
Department of Mechanical Engineering and Materials Science, University of Pittsburgh, Pittsburgh, PA,USA 15261

Abstract

Currently a telerehabilitation system includes a therapist and a patient where the therapist interacts with the patient, typically via a verbal and visual communication, for assessment and supervision of rehabilitation interventions. This mechanism often fails to provide physical assistance, which is a modus operandi during physical therapy or occupational therapy. Incorporating an actuation modality such as functional electrical stimulation (FES) or a robot at the patient's end that can be controlled by a therapist remotely, to provide therapy or to assess and measure rehabilitation outcomes can significantly transform current telerehabilitation technology. In this paper, a position-synchronization controller is derived for FES-based telerehabilitation to provide physical assistance that can be controlled remotely. The newly derived controller synchronizes an FES-driven human limb with a remote physical therapist's robotic manipulator despite constant bilateral communication delays. The control design overcomes a major stability analysis challenge: the unknown and unstructured nonlinearities in the FES-driven musculoskeletal dynamics. To address this challenge, the nonlinear muscle model was estimated through two neural networks functions that approximated unstructured nonlinearities and an adaptive control law for structured nonlinearities with online update laws. A Lyapunov-based stability analysis was used to prove the globally uniformly ultimately bounded tracking performance. The performance of the state synchronization controller was validated through experiments on an able-bodied subject. Specifically, we demonstrated bilateral control of FES-elicited leg extension and a human operated robotic manipulator. The controller was shown to effectively synchronize the system despite unknown and different delays in the forward and backward channels.

Correspondence to: Nitin Sharma.

1 Introduction

Neurological impairments due to stroke are the leading causes of disability in the United States. Over 795,000 individuals are affected by stroke each year [1]. Loss of limb function hinders activities of daily living (ADL), significantly limits long-term independence [2], and increases dependency on the United States (US) healthcare system; thus, burdening the US economy. The maximum recovery of limb function occurs at around 6 months after a stroke and begins to decline as soon as 1 year post stroke [3]. To facilitate ADL, the goal of therapy is to strengthen and stretch muscles and to retrain the central nervous system to voluntarily activate the limb muscles. Rehabilitation involves numerous hours of repetitive physical exercises that are provided by trained therapists. However, due to reasons such as limited number of community rehabilitation service providers, repetitious nature of the therapy, and increasing labor cost, survivors' ability to maintain and improve the gains in limb function 6 months after the stroke becomes limited. In addition, the inconvenience associated with getting to the clinic after discharge is often the main barrier to obtain rehabilitation services. Therefore, it is critical to determine the most effective and efficient way to deliver rehabilitation services after stroke. Aforementioned issues and a likely significant rise in the number of patients in the future have led to the emergence of alternative means to impart physical therapy. For example, functional electrical stimulation (FES), therapy robots, and in-home rehabilitation services called telerehabilitation have been proposed to provide therapeutic exercises.

Telerehabilitation is the application of rehabilitation services where a patient and a therapist interact via a telecommunication medium. Currently, telerehabilitation is used for patient assessment, consultation, supervision, and management [4,5]. Telerehabilitation has been found to be just as feasible as standard in-clinic therapy and is even preferred by the participating therapists and patients [6]. A survey of telemedicine applications which include: physical therapy, occupational therapy, speech and language pathology assessments, etc. was discussed in [7]. A number of video-conferencing-based physical therapy and occupational therapy cases including patients with multiple sclerosis, knee osteoarthritis, bronchopulmonary dysplasia, stroke, and Parkinson disease were reported. In all of the cases significant improvements and benefits to patients who lived far or preferred in-home service delivery were reported. In [8] the results from a clinical study on upper extremity telerehabilitation was presented. Thirteen participants with spinal cord injury were used to compare two FES-based telerehabilitation treatment methods: 1) conventional exercise therapy and 2) ReJoyce exercise therapy with a telesupervisor. The therapist supervised the subjects through a two-way verbal and video communication. The internet-based ReJoyce system was shown to induce statistically and clinically significant hand strength improvements compared to conventional therapy. In [9], the study examined the efficacy of an FES program administered via the Ness H200 Hand rehabilitation system (Bioness Inc., Valencia, CA). The study involved only video and verbal communication between a therapist and one patient with stroke. The participant's ability to perform ADL increased after the internet therapy and the affected upper-extremity impairment also decreased after the therapy was over. A web-based telerehabilitation system for upper extremity rehabilitation that used a force feedback joystick and Java therapy software was demonstrated in [10]. The exercise data was collected from a subject with chronic stroke. It was demonstrated that the system can organize a therapy program, engage a user, and track improvements due to therapy. In a similar but preceding study, the RM-II hand Master glove was used for force feedback in a virtual reality based telerehabilitation system [11]. In [12] a closed-loop telerehabilitation system for restoring hand function and recording emotional state of a user was tested. FES was used to assist hand opening and closing. The feedback to FES was provided by a Microsoft Kinect sensor. At the same time facial expressions of persons with stroke were recorded and analyzed for emotional response of the subjects during FES. The Kinect sensor was shown to successfully control opening and closing of hand but facial expression recognition was found to be unreliable.

These telerehabilitation platforms lack a medium to provide external physical assistance. Incorporating an actuation modality such as FES or a robot at the patient's end, which mimics a therapist in a remote clinic, may be necessary for therapeutic purposes until the patient's recovery is maximized. Although a robot guided rehabilitation intervention is a feasible option, it might be more therapeutically beneficial to include functional electrical stimulation (FES). FES is a treatment where a skeletal muscle can be activated by passing low-level electric currents across the motor neurons. This treatment can be administered by applying transcutaneous electrodes over the surface of the skin. The reason why FES is helpful is because it can strengthen muscle, prevent muscle atrophy, and increase bone density. Moreover, FES has neuroplastic effects as it helps to retrain active motor units and rebuild the weak connections between the brain and the motor neurons [13, 14]. The current rehabilitation systems that simply stretch muscles or move limbs through a range of motion provide only part of the needed therapy and hence, may not be as beneficial as FES. Therefore, due to its physiological advantages, FES is an added benefit during telerehabilitation of persons with partial or complete loss of limb function [15].

In a review on telerehabilitation, Carignan and Krebs [16] pointed out that the closed-loop control of bilateral robotic telerehabilitation is challenging due to limited bandwidth, data losses, and transmission delays in a communication network. These effects degrade the quality of physical interaction and may destabilize a remote session. Designing a controller that compensates for bilateral delays during a telerehabilitation system that uses FES is further complicated by uncertain and highly nonlinear musculoskeletal dynamics. Due to the uncertain nonlinear muscle behavior during FES, recently many nonlinear techniques including neural network-based adaptive FES controllers have been proposed [17–24]. Some of these controllers have been designed using Lyapunov-based stability analysis and the controller stability is usually guaranteed despite uncertainties and nonlinearities. Control of bilateral control of teleoperated robots on the other hand has received tremendous attention (see [25–28] and references therein). However, very few researchers have looked at designing a bilateral telerehabilitation controller for FES and a robot along with stability guarantees. An FES-based system was used to synchronize a master human arm and a slave human arm in [29], where a simple PID controller was used to modulate the FES. However, no stability guarantees were provided in the presence of model uncertainties and time delays. In [30] an FES-based bilateral teleoperation controller with stability guarantees was developed. The controller synchronized the positions of a patient's arm, which was activated by FES, and a master robot, which was controlled by a therapist. The proposed therapy method contained the benefits of FES, while incorporating the conveniences of telerehabilitation. In [31], a delay compensation controller developed in [32] to counteract the electromechanical delay associated with FES and a communication delay, was experimentally tested on a human arm. However, that controller was not developed to account for the communication delay in the feedback to a master robot.

Motivated to address the aforementioned gaps, we propose a telerehabilitation setup that uses a leg extension machine to train the upper leg through FES. The FES is used to interact with the subject remotely. Potentially, this telerehabilitation set up can be used as a muscle building intervention and as subjects have improvements due to neuroplasticity or their muscle strength improves, the proposed neural network-based framework can potentially adapt the therapy. This paper is an extension of our previous work [30, 31]. In this paper, the controller is further refined to improve the effectiveness of the neural networks by modifying the error structure and most importantly, the controller was validated through experiments on an able-bodied subject. Further, we assume that the robot dynamics are uncertain, but linearly parameterizable and the musculoskeletal dynamics has structured and unstructured nonlinearities. Therefore, a feedforward adaptive controller was used for the robot dynamics and two single layer feedforward neural networks and an adaptive control law was used for the musculoskeletal system. The two single layer neural networks were used to model the unstructured nonlinear passive and active muscle dynamics and the adaptive control law was used for the structured nonlinearties. The state synchronization controller was able to achieve a globally uniformly ultimately bounded (GUUB) state synchronization in the presence of communication delays and environmental forces.

2 System Dynamics

As shown in Fig. 1, the telerehabilitation system consists of a robotic manipulator controlled by a human operator and an FES driven musculoskeletal system. The dynamics of the n-link robotic manipulator are given by

$$M_r(q_r)\ddot{q}_r+C_r(q_r,\dot{q}_r)\dot{q}_r+G_r(q_r)=F_h+\tau_r, \quad (1)$$

where q_r, $\dot{q}_r$, $\ddot{q}_r \in \mathbb{R}^n$ denote the angular position, velocity, and acceleration about each joint, respectively. In (1), $M_r \in \mathbb{R}^{n\times n}$ denotes the positive definite inertia matrix, $C_r \in \mathbb{R}^{n\times n}$ denotes the Centripetal/Coriolis matrix, $G_r \in \mathbb{R}^n$ denotes the gravitational torques, and $\tau_r(t) \in \mathbb{R}^n$ denotes the motor torque acting on each joint. In (1), $F_h(t) \in \mathbb{R}^n$ denotes the torque created by the human operator applying a force on the robot. In order to develop the controller, this torque is assumed to be applied by the human operator and is modeled as a PD controller which can be expressed as

$$F_h(t)=K_pe_d+K_d\dot{e}_d, \quad (2)$$

where K_p, $K_d \in \mathbb{R}^+$ are the unknown proportional and derivative control gains and e_d is the user driven error and is defined as the difference between the desired robot position based on the operators intent and the actual robot position, $e_d = q_d - q_r$. The desired trajectory, $q_d \in \mathbb{R}^n$, is the motion planned for the robot and subject and is fully controlled by the human operator. To facilitate the control development the unknown gains K_p and K_d can be defined as $K_p = \alpha_d \lambda_d$ and $K_d = \alpha_d$, where $\alpha_d, \lambda_d \in \mathbb{R}^+$ are unknown constants and are assumed to be upper bounded by $\bar{\alpha}_d, \bar{\lambda}_d \in \mathbb{R}^+$, which allows F_h to be expressed as

$$F_h(t) = \alpha_d(\bar{q}_d - \bar{q}_r), \quad (3)$$

where $\bar{q}_d, \bar{q}_r \in \mathbb{R}^n$ are defined as $\bar{q}_r = \dot{q}_r + \lambda_d q_r$ and $\bar{q}_d = \dot{q}_d + \lambda_d q_d$. The desired position and velocity are bounded i.e., $q_d, \dot{q}_d \in \mathcal{L}_\infty$: Because q_d is a designed trajectory, it can be shown that $\alpha_d \|\bar{q}_d\| \le \xi$ where $\xi \in \mathbb{R}^+$ is a constant.

Remark 1

The desired trajectory, q_d, is the motion planned by the human operator for the robotic manipulator and the FES system. Therefore, a therapist can customize the trajectories based on prior knowledge of the patient's range of motion and observations made during therapy sessions.

The FES driven musculoskeletal system dynamics are represented as:

$$J(q_s)\ddot{q}_s + C_s(q_s, \dot{q}_s)\dot{q}_s + M_\upsilon(\dot{q}_s) + M_e(q_s) + M_g(q_s) + d(t) = \Gamma_s(t) - F_e(t), \quad (4)$$

$$\Gamma_s(t) = F_m \zeta^T(q_s)\eta(q_s, \dot{q}_s)u(t), \quad (5)$$

where $q_s, \dot{q}_s, \ddot{q}_s \in \mathbb{R}^n$ denote the angular position, velocity, and acceleration about each joint, respectively. In (4), $J \in \mathbb{R}^{n \times n}$ denotes the unknown inertia of a limb fixed in a test apparatus, $C_s \in \mathbb{R}^{n \times n}$ denotes the Centripetal/Coriolis matrix, $M_e \in \mathbb{R}^n$ denotes the moment generated by the passive elastic properties of the muscles, $M_\upsilon \in \mathbb{R}^n$ denotes the moment generated by the passive viscous properties of the muscles, $M_g \in \mathbb{R}^n$ denotes the gravitational torque acting on the limb, and $d(t) \in \mathbb{R}^n$ denotes any disturbances that may arise in the system. For detailed definitions of M_e, M_υ, and M_g, see [33]. The input to the FES system, $\Gamma_s(t) \in \mathbb{R}^n$, is the torque produced using FES, and $F_e(t) \in \mathbb{R}^n$ is the interaction force between the musculoskeletal system and environment. In (5), $F_m \in \mathbb{R}^n$ denotes the constant maximum isometric force generated by the muscle, $\zeta \in \mathbb{R}^n$ denotes a positive moment arm that changes with respect to the joint angle, and $\eta \in \mathbb{R}^{n \times n}$ denotes an unknown nonlinear function of the muscle force-length and force-velocity relationships.

The normalized voltage to induce muscle contractions is denoted as $u \in \mathbb{R}^n$ and is modeled by a piecewise linear function, also known as the recruitment curve [34], as

$$u(t)=\mathrm{sat}[\upsilon(t)]=\begin{cases} 0 & \upsilon<\upsilon_{\min} \\ \frac{\upsilon(t)-\upsilon_{\min}}{\upsilon_{\max}-\upsilon_{\min}} & \upsilon_{\min}\le\upsilon\le\upsilon_{\max} \\ 1 & \upsilon>\upsilon_{\max} \end{cases} \quad (6)$$

where $\upsilon_{min} \in \mathbb{R}^n$ is the minimum voltage required to produce a tensioning in the muscle and $\upsilon_{max} \in \mathbb{R}^n$ is the minimum voltage at which there is no considerable increase in force or movement observed or the maximum voltage level the subject is comfortable with. In (6), the applied stimulation voltage is denoted as $\upsilon \in \mathbb{R}^n$. For the sake of simplifying the control structure and derivations, the muscle activation dynamics are neglected in this model. In this paper we explore the scenario where the environmental interaction force in (4), F_e, is modeled as a passive force proportional to the position and velocity and is defined as

$$F_e(t)=\alpha_s(\dot{q}_s+\lambda q_s), \quad (7)$$

where α_s, $\lambda \in \mathbb{R}^+$ are unknown constants and α_s is bounded by $\bar{\alpha}_s \in \mathbb{R}^+$.

3 Control Development

The control objective is to design a set of controllers that can achieve state synchronization between the robotic manipulator and musculoskeletal system over a network in the presence of telecommunication delays. In realistic networked control systems, time delays in the forward and backward path are typically different since data packets may go through different network paths [35]. Therefore, the position errors are defined as [27]

$$e_r(t)=q_s(t-t_{sr})-q_r(t),$$

$$e_s(t)=q_r(t-t_{rs})-q_s(t),$$

where t_{sr}, $t_{rs} \in \mathbb{R}^+$ are unknown delays in the communication network on the robotic manipulator's end and musculoskeletal system's end, respectively. To facilitate the stability analysis the following auxiliary errors are defined as

$$r_r=\dot{e}_r+\lambda_r e_r,$$

$$r_s=\dot{e}_s+\lambda_s e_s,$$

where λ_r, $\lambda_s \in \mathbb{R}^+$ are control gains. The robotic manipulator will be controlled using an adaptive control algorithm to estimate the unknown parameters of the robot. The musculoskeletal system will be controlled using an adaptive and nonlinear neural network based control algorithm in order to estimate the nonlinear and uncertain muscle dynamics.

Notations/Assumptions

To simplify the control development, the following notations and assumptions are used:

- The function of time notation is dropped (e.g., $e(t) \rightarrow e$) and any delayed term is denoted by a subscript (e.g., $e(t - t_d) \rightarrow e_{t_d}$).
- The Forbenius norm of a matrix is denoted as $\|\|_F$.
- The function, $\Omega(q_s, \dot{q}_s) \in \mathbb{R}^{n \times n}$, is introduced and is defined as $\Omega = F_m \zeta^T \eta$, where F_m, ζ, and η were introduced in (5). Further, it is assumed that $\|\Omega\|_F \geq \bar{\Omega} \in \mathbb{R}^+$ in order to justify bounding the second neural network. This assumption is justified because of the physical properties of the muscles. The muscle tension will only drop to zero when the muscle is at full length and is considerably reduced but not zero when fully shortened [36]. The range of motion of the limb will ensure that the muscle is never fully lengthened, therefore the force-length relationship never drops to zero. The force-velocity relationship is bounded by a non-zero number since it only equals zero when the muscle shortening velocity is near its maximum which is outside the range of the velocities imposed in this control problem. Note that the first time derivative of Ω is not assumed nor required to be bounded, unlike our earlier papers [17, 33].
- It is assumed that the structured nonlinearities of the robot and musculoskeletal dynamics are linearly parameterizable, (e.g., $Y\theta = M\dot{q} + C\dot{q} - G$), where $\theta \in \mathbb{R}^p$ is the vector that contains the p-unknown parameters and $Y \in \mathbb{R}^{n \times p}$ is the regression matrix.
- The disturbance term in the musculoskeletal dynamics, $d(t)$, is bounded by a constant such that $\|d\| \leq \bar{d}$ where $\bar{d} \in \mathbb{R}^+$ is a constant.

3.1 Closed Loop Robotic System

The closed loop error system for the robotic manipulator is developed by multiplying the time derivative of r_r by M_r resulting in

$$M_r \dot{r}_r = M_r \ddot{e}_r + \lambda_r M_r \dot{e}_r.$$

After substituting in the robot dynamics from (1) and adding and subtracting $C_r r_r$, the result becomes

$$M_r \dot{r}_r + C_r r_r = Y_r \theta_r - \alpha_d \overline{q}_d - \tau_r, \quad (8)$$

where the linearly parameterizable terms in the dynamics are grouped into $Y_r \theta_r$ as

$$Y_r \theta_r = M_r \ddot{q}_{st_{sr}} + \alpha_d \overline{q}_r + C_r (\dot{q}_r + r_r) + G_r + \lambda_r M_r \dot{e}_r.$$

The control input for the robotic manipulator is defined as

$$\tau_r(t)=\overline{\tau}_r(t)+Y_r\hat{\theta}_r, \quad (9)$$

where $Y_r\hat{\theta}_r$ is an estimate of the linearly parameterizable robot dynamics, $Y_r\theta_r$, and $\bar{\tau}_r(t)$ is the coordinated torque for the robot, which is defined as

$$\overline{\tau}_r=k_r r_r, \quad (10)$$

where $k_r \in \mathbb{R}^+$ is a control gain. Although the communication delay is unknown, substituting (9) into (8) results in

$$M_r\dot{r}_r+C_r r_r=Y_r\tilde{\theta}_r-\alpha_d\overline{q}_d-\overline{\tau}_r, \quad (11)$$

where $\tilde{\theta}_r = \theta_r - \hat{\theta}_r$ is defined as the parameter estimation error. The update law used to modify the parameter estimation vector is defined as

$$\dot{\hat{\theta}}_r=\mathrm{proj}(\Gamma_1\, Y_r^T r_r), \quad (12)$$

where $\Gamma_1 \in \mathbb{R}^{p \times p}$ denotes a positive definite gain matrix.

3.2 Closed Loop Musculoskeletal System

The closed loop system for the musculoskeletal dynamics is developed by multiplying the time derivative of r_s by J, using (4), and adding the term $C_s r_s$ to both sides of the equation resulting in

$$J\dot{r}_s+C_s r_s=J\ddot{q}_{rt_{rs}}+C_s(\dot{q}_s+r_s)+M_v+M_e+M_g+d-\Omega u+F_e+\lambda_s J\dot{e}_s. \quad (13)$$

The unknown nonlinear terms in (13) are lumped into the auxiliary function $f(q_s, \dot{q}_s)$ and the linearly parameterized term $Y_s\theta_s$, defined as

$$f=M_v+M_e+M_g+C_s\dot{q}_s+\alpha_s(\dot{q}_s+\lambda q_s), \quad (14)$$

$$Y_s\theta_s=J\ddot{q}_{rt_{rs}}+\lambda_s J\dot{e}_s+C_s r_s. \quad (15)$$

Expression (13) can be written as

$$J\dot{r}_s+C_s r_s=f+Y_s\theta_s-\Omega u+d. \quad (16)$$

The control law is designed as

$$u=\Psi^{-1}\left(\bar{u}+\hat{f}+Y_s\hat{\theta}_s\right), \quad (17)$$

where $Y_s\hat{\theta}_s$ is an estimate of the linearly parameterizable terms in $Y_s\theta_s$ and Ψ is defined as

$$\Psi=\left(\hat{\Omega}+\left(\varrho(\hat{\Omega})+\beta\right)I_{n\times n}\right). \quad (18)$$

To avoid a singularity when $\hat{\Omega}$ is equal to zero, the spectral radius of $\hat{\Omega}$, $\varrho(\hat{\Omega}) \in \mathbb{R}^+$, and a control gain, $\beta \in \mathbb{R}^+$, are added to Ψ [37]. The additional feedback based input, $\bar{u} \in \mathbb{R}^n$, is defined as

$$\bar{u}=k_s r_s, \quad (19)$$

where $k_s \in \mathbb{R}^+$ is a control gain.

In (17) and (18), $\hat{f} \in \mathbb{R}^n$ and $\hat{\Omega} \in \mathbb{R}^{n\times n}$ denote an approximation of the auxiliary function, f, and the muscle dynamics function, Ω, which are represented by two single layered neural networks (NN) as

$$f=W^T\sigma(y)+\varepsilon_1(y), \quad (20)$$

$$\Omega=R^T\phi(y)+\varepsilon_2(y). \quad (21)$$

The input to the NN's is the augmented input vector $y \in \mathbb{R}^{2n+1}$ defined as $y = [1\ q_s\ \dot{q}_s]$. The ideal weight matrices for the two neural networks are denoted as $W \in \mathbb{R}^{N_f\times n}$ and $R \in \mathbb{R}^{N_\Omega\times n}$. The input layer is comprised of $2n + 1$ neurons, N_f and N_Ω are the number of neurons in the hidden layer for the NN's, and n is the number of neurons in the output layer. The activation function for the first NN that maps the input layer to the hidden layer is denoted as $\sigma : \mathbb{R}^{2n+1} \to \mathbb{R}^{N_f}$. The activation function for the second NN that maps the input layer to the output layer is denoted as $\phi : \mathbb{R}^{2n+1} \to \mathbb{R}^{N_\Omega\times n}$. The unknown functional reconstruction errors for the two NN's are denoted as $\varepsilon_1 \in \mathbb{R}^n$ and $\varepsilon_2 \in \mathbb{R}^{n\times n}$ and are bounded, i.e., $\|\varepsilon_1\| \leq \bar{\varepsilon}_1$ and $\|\varepsilon_2\| \leq \bar{\varepsilon}_2$ where $\bar{\varepsilon}_1, \bar{\varepsilon}_2 \in \mathbb{R}^+$, respectively. The estimates of the ideal NN's that approximate f and Ω are denoted as

$$\hat{f}=\hat{W}^T\sigma(y), \quad (22)$$

$$\hat{\Omega}=\hat{R}^T\phi(y), \quad (23)$$

where $\hat{W}\in\mathbb{R}^{N_f\times n}$ and $\hat{R}\in\mathbb{R}^{N_\Omega\times n}$ are the estimates of the ideal weights. Adding and subtracting Ψ_υ to (16) and using (17) results in

$$J\dot{r}_s+C_s r_s=\tilde{f}+Y_s\tilde{\theta}_s-\tilde{\Omega}u+d-\bar{u},$$

where the functional estimation errors are defined as $\tilde{f}=f-\hat{f}$ and $\tilde{\Omega}=\Omega-\Psi$ and $\tilde{\theta}_s=\theta_s-\hat{\theta}_s$, is the parameter estimation error. After using some of the neural network properties [38] the functional estimation errors, $\tilde{\Omega}$ and $\tilde{f}$, can be expressed as

$$\tilde{f}=\tilde{W}^T\sigma+\varepsilon_1,$$

$$\tilde{\Omega}=\tilde{R}^T\phi+\beta_\varepsilon,$$

where the network disturbance for the NN's are ε_1 and $\beta_\varepsilon=\varepsilon_2-(\varrho(\hat{\Omega})+\beta)I_{n\times n}$ and β_ε is bounded by $\overline{\beta}_\varepsilon\in\mathbb{R}^+$ (i.e., $\|\beta_\varepsilon\|_F\le\overline{\beta}_\varepsilon$). The weight estimation errors are defined as $\tilde{W}=W-\hat{W}$ and $\tilde{R}=R-\hat{R}$. Based on the subsequent stability analysis, the update laws, to modify the weights for each layer, are defined as

$$\dot{\hat{\theta}}_s=\mathrm{proj}(\Gamma_2 Y_s^T r_s),$$

$$\dot{\hat{W}}=\mathrm{proj}\ (\Gamma_3\sigma r_s^T), \quad (24)$$

$$\dot{\hat{R}}=\mathrm{proj}\ \left(-\Gamma_4\phi u r_s^T\right),$$

where $\Gamma_2\in\mathbb{R}^{g\times g}$, $\Gamma_3\in\mathbb{R}^{N_f\times N_f}$, and $\Gamma_4\in\mathbb{R}^{N_\Omega\times N_\Omega}$ are positive definite gain matrices where $g\in\mathbb{R}^+$ is the number of unknown parameters in θ_s. The update laws use the projection algorithm, *proj*, to ensure that the weights are bounded [39], therefore NN's are bounded as $\|\hat{f}\|\le\Upsilon_1$ and $\|\Psi^{-1}\|_F\le\Upsilon_2$ where $\Upsilon_1,\Upsilon_2\in\mathbb{R}^+$ are known constants. The final closed loop system for the FES system is

$$J\dot{r}_s=-C_s r_s+\tilde{W}^T\sigma+Y_s\tilde{\theta}_s-\left(\tilde{R}^T\phi+\beta_\varepsilon\right)u+\varepsilon_1+d-\bar{u}, \quad (25)$$

4 Stability Analysis

Theorem 1

Consider the nonlinear FES-based bilateral telerehabilitation system described in (1)–(7). *In the presence of unknown constant communication delays all the signals in the system are globally uniformly ultimately bounded (GUUB) using the control inputs defined in* (9) *and* (17), *and the update laws defined in* (12) *and* (24) *provided the following gain conditions hold true:*

$$k_r > \frac{1}{2} + \frac{1}{2\upsilon_1}, k_s > \frac{1}{2} + \frac{1}{2\upsilon_2}, \lambda_r > \frac{1}{2}, \lambda_s > \frac{1}{2}$$

where υ_1 *and* $\upsilon_2 \in \mathbb{R}^+$ *are subsequently defined arbitrary constants.*

Proof—A positive definite Lyapunov candidate $V(x, t) \in \mathbb{R}$ is defined as

$$V \triangleq \frac{1}{2} r_r^T M_r r_r + \frac{1}{2} r_s^T J r_s + \frac{1}{2} e_r^T e_r + \frac{1}{2} e_s^T e_s + \frac{1}{2} \tilde{\theta}_r^T \Gamma_1^{-1} \tilde{\theta}_r + \frac{1}{2} \tilde{\theta}_s^T \Gamma_2^{-1} \tilde{\theta}_s + \frac{1}{2} \mathrm{tr} \left\{ \tilde{W}^T \Gamma_3^{-1} \tilde{W} \right\} + \frac{1}{2} \mathrm{tr} \left\{ \tilde{R}^T \Gamma_4^{-1} \tilde{R} \right\}. \quad (26)$$

Since the projection algorithm [39] is being used to bound $\hat{\theta}_r$, $\hat{\theta}_s$, $\hat{W}$, and $\hat{R}$ to within a certain range, the Lyapunov candidate can be upper and lower bounded as

$$\lambda_{\min} \|x\|^2 \le V \le \lambda_{\max} \|x\|^2 + \psi, \quad (27)$$

where λ_{min}, λ_{max}, $\psi \in \mathbb{R}^+$ are known constants and $x \in \mathbb{R}^{4n}$ is defined as

$$x = \begin{bmatrix} r_r^T & r_s^T & e_r^T & e_s^T \end{bmatrix}^T. \quad (28)$$

After using (11) and (25) the time derivative of $V(x, t)$ can be written as

$$\begin{aligned} \dot{V} = & \frac{1}{2} r_r^T \dot{M}_r r_r + r_r^T \left(-C_r r_r + Y_r \tilde{\theta}_r - \alpha_d \overline{q}_d - \overline{\tau}_r \right) + \frac{1}{2} r_s^T \dot{J} r_s \\ & + r_s^T \left(-C_s r_s + \tilde{W}^T \sigma + Y_s \tilde{\theta}_s - \left(\tilde{R}^T \phi + \beta_\varepsilon \right) u + \varepsilon_1 + d - \bar{u} \right) \\ & + e_r^T \dot{e}_r + e_s^T \dot{e}_s + \tilde{\theta}_r^T \Gamma_1^{-1} \dot{\tilde{\theta}}_r + \tilde{\theta}_s^T \Gamma_2^{-1} \dot{\tilde{\theta}}_s \\ & - \mathrm{tr} \left\{ \tilde{W}^T \Gamma_3^{-1} \dot{\hat{W}} \right\} \\ & - \mathrm{tr} \left\{ \tilde{R}^T \Gamma_4^{-1} \dot{\hat{R}} \right\} \end{aligned} \quad (29)$$

Regrouping the neural network terms in (29) into the $tr\{\}$ function results in

$$\dot{V}=\frac{1}{2}r_r^T\dot{M}_r r_r+r_r^T(-C_r r_r+Y_r\tilde{\theta}_r-\alpha_d\overline{q}_d-\overline{\tau}_r$$
$$+\frac{1}{2}r_s^T\dot{J}r_s+r_s^T(-C_s r_s+Y_s\tilde{\theta}_s-\beta_\varepsilon u+\varepsilon_1+d-\bar{u}$$
$$+e_r^T\dot{e}_r+e_s^T\dot{e}_s-\tilde{\theta}_r^T\Gamma_1^{-1}\dot{\hat{\theta}}_r+\tilde{\theta}_s^T\Gamma_2^{-1}\dot{\hat{\theta}}_s$$
$$-\text{tr}\left\{\tilde{W}^T\left(\Gamma_3^{-1}\dot{\hat{W}}-\sigma r_s^T\right)\right\}-\text{tr}\left\{\tilde{R}^T\left(\Gamma_4^{-1}\dot{\hat{R}}+\phi u r_s^T\right)\right\} \quad (30)$$

By using the update laws (24) and (12), canceling out the similar terms, and using the skew symmetry property $\left(r_r^T[\dot{M}_r-2C_r]r_r=0\right)$ and $\left(r_s^T[\dot{J}-2C_s]r_s=0\right)$, (30) can be written as

$$\dot{V}=r_r^T(-\alpha_d\overline{q}_d-\overline{\tau}_r)+r_s^T(-\beta_\varepsilon u+\varepsilon_1+d-\overline{v})+e_r^T\dot{e}_r+e_s^T\dot{e}_s$$

Using (10), (19) we obtain

$$\dot{V}=r_r^T(-\alpha_d\overline{q}_d-k_r r_r)+r_s^T(-k_s r_s-\beta_\varepsilon u+\varepsilon_1+d)+e_r^T(r_r-\lambda_r e_r)+e_s^T(r_s-\lambda_s e_s)$$

Using (2), (7), and (17) the previous equation can be rearranged to

$$\dot{V}=k_r r_r^T r_r-k_s r_s^T r_s-\lambda_r e_r^T e_r-\lambda_s e_s^T e_s+e_r^T r_r+e_s^T r_s-\alpha_d r_r^T\overline{q}_d+r_s^T(-\beta_\varepsilon u+\varepsilon_1+d) \quad (31)$$

By using the following inequalities

$$\left\|\alpha_d r_r^T\overline{q}_d\right\|\leq\xi\|r_r\|,$$

$$\left\|r_s^T(-\beta_\varepsilon u+\varepsilon_1+d)\right\|\leq(\overline{\beta}_\varepsilon+\overline{\varepsilon}_1+\overline{d})\|r_s\|$$

$$\left\|e_r^T r_r\right\|\leq\frac{1}{2}\|e_r\|^2+\frac{1}{2}\|r_r\|^2,$$

$$\left\|e_s^T r_s\right\|\leq\frac{1}{2}\|e_s\|^2+\frac{1}{2}\|r_s\|^2,$$

(31) can be upper bounded as

$$\dot{V} \leq -\left(k_r - \frac{1}{2}\right) r_r^T r_r - \left(k_s - \frac{1}{2}\right) r_s^T r_s - \left(\lambda_r - \frac{1}{2}\right) e_r^T e_r - \left(\lambda_s - \frac{1}{2}\right) e_s^T e_s + (\overline{\beta}_\varepsilon + \overline{\varepsilon}_1 + \overline{d})\|r_s\| + \xi\|r_r\|. \quad (32)$$

After using nonlinear damping [40], (32) can be further upper bounded as

$$\dot{V} \leq -\frac{1}{2} K_{\min}\|x\|^2 + \frac{\xi^2}{2\upsilon_1} + \frac{(\overline{\beta}_\varepsilon + \overline{\varepsilon}_1 + \overline{d})^2}{2\upsilon_2} \quad (33)$$

where $\upsilon_1, \upsilon_2 \in \mathbb{R}^+$ are constants and

$$K_{\min} = \min\left\{k_r - \frac{1}{2} - \frac{1}{2\upsilon_1}, k_s - \frac{1}{2} - \frac{1}{2\upsilon_2}, \lambda_r - \frac{1}{2}, \lambda_s - \frac{1}{2}\right\}.$$

(33) can be further bounded to yield

$$\dot{V} \leq -\frac{1}{2} K_{\min}\|x\|^2 + A, \quad (34)$$

where $A = \frac{\xi^2}{2\upsilon_1} + \frac{(\overline{\beta}_\varepsilon + \overline{\varepsilon}_1 + \overline{d})^2}{2\upsilon_2}$. Adding and subtracting $\frac{1}{2}\frac{K_{\min}}{\lambda_{\max}}\psi$ to (34) and using (27), the following expression is obtained

$$\dot{V} \leq -\frac{1}{2}\frac{K_{\min}}{\lambda_{\max}} V + B, \quad (35)$$

where $B = \frac{1}{2}\frac{K_{\min}}{\lambda_{\max}}\psi + A$. (35) can be integrated to obtain:

$$V(x,t) \leq V(0) e^{-\frac{1}{2}\frac{K_{\min}}{\lambda_{\max}}t} + B\left(1 - e^{-\frac{1}{2}\frac{K_{\min}}{\lambda_{\max}}t}\right). \quad (36)$$

From (36) it is evident that $V(x, t)$ decays exponentially to a bound B which can be minimized using the control gains. Since $V \in \mathcal{L}_\infty$ the states $r_r, r_s, e_r, e_s \in \mathcal{L}_\infty$. Further analysis can be done to show that the $\|x\|$ decays to the ball of radius $\sqrt{\frac{2B}{\lambda_{\min}}}$. By Theorem 4.18 in [40], it can be concluded that the origin of x is GUUB.

5 Experiments

Experiments were conducted on an able-bodied subject (male, age: 21 years) after obtaining approval from the University of Pittsburgh Institutional Review Board. The experiments staged a telerehabilitation session where a therapist's robot interacted with the participant's upper leg through FES. The proposed controller was used to synchronize position of the robotic manipulator and the subject's upper leg despite unknown communication delays. We tested three scenarios: 1) the participant's intentional movements are mimicked by the robot; i.e., the robot acts as a slave and tracks a delayed leg angle trajectory, 2) a human operator uses the robot to manipulate the participant's leg via FES; i.e., the leg acts as a slave and tracks a delayed robot angle trajectory, and 3) an interactive experiment where the participant's intentional movements can be halted by the human operator.

5.1 Testbed

The experiments were performed on a testbed that consisted of a modified leg extension machine (LEM) and a Phantom Omni robot (Geomagic Inc, USA) was used as a manipulator for a human operator. The LEM was modified with an incremental optical encoder (Hengxiang, CN) with a resolution of 1024 pulses per revolution to measure the knee joint angle. Resistance bands were added to the LEM to create the passive environment torque, F_e in (7). The Phantom Omni robot has 3 motorized degrees of freedom, but only one link was used to manipulate the leg and its other two links were kept fixed. A RehaStim 8-channel stimulator (Hasomed Inc., DE) was used for stimulating the quadriceps muscle. A current modulated biphasic stimulation scheme was used at a frequency of 35 Hz with a 400μs pulse width. A pair of transcutaneous electrodes (AxelGaard Manufacturing Co., USA) were placed on the quadriceps muscle: one near the knee joint and another distal to the first electrode. A QPIDe (Quanser Inc, Ontario Canada) DAQ board was used to interface with the sensors and run the controller in real-time at 1 kHz. The control algorithms were coded in Simulink (MathWorks Inc, USA) and implemented using the Quarc real-time software (Quanser Inc, Ontario Canada) running on a Windows machine (Intel Xeon 3.10 GHz processor). The controller for the robotic manipulator and FES system were both implemented in a single program and an artificial transmission delay of 50ms was coded between the robot and FES (forward channel) and a 80ms delay was coded between FES and the robot (backward channel). These network delays were chosen to simulate a higher quality internet connection on the therapist's end and lower quality connection on the patient's end.

5.2 Offline Training of Neural Network

The proposed controller uses the NNs to approximate the functions in (20) and (21). The controller then adapts the weights online using a single step learning basis, i.e., the weights are adapted each time step based on the current errors. While the controller in (17) does not require offline training of the NNs, running the controller with a cold start/random initial weights for the NN may not be practical. Therefore, the NNs were pre-trained offline to find a reasonable starting point for the NN weights which also use online adaptive laws in (24) during the experiments. Because the NNs are being used to approximate functions that are not measurable, training through batch processing based on subject recorded data is not possible. Therefore, a musculoskeletal model with able-bodied subject parameters, taken from [41], was used to generate the terms that would be approximated by the NNs. Then a back propagation algorithm [38] was used to train the NNs offline. The functions in (20) and (21) are dependent on the limb position and velocity; therefore, a set of data was generated from 8 sinusoidal movements with different time periods. This ensured that the NN were being trained for a variety of possible limb positions and velocities. This tuning process not only finds the initial starting point for the weights, $\hat{W}$ and $\hat{R}$, but also the rate and bias parameters of the activation functions, σ and ϕ.

5.3 Experimental Protocol and Results

As described before, three sets of experiments were conducted on an able-bodied subject. In the first set of experiments, the test subject takes the role of the master by voluntarily extending his leg, the controller then forces the robotic manipulator to track his leg movements. In this setup the test subject was instructed to move his leg in three different ways: step, ramp, and sinusoidal. The delayed subject's knee angle and the robot link angle and the input to the robot and FES for the three trials are plotted in Fig. 3.

In the second set of experiments the driving force of the system was the human operator who manipulated the robot, which acted as a master and the subject's leg, which acted as a slave, tracked the robot's delayed trajectory. The human operator attempted to reproduce the same three movement types:, as in the first set of experiments, step, ramp, and sinusoidal. The delayed robot link angle and subject's knee angle and the input to the robot and FES for the three trials are plotted in Fig. 3. From the plots, it can be observed that there was a steady state error. This is to be expected because there is no integral control, and the NN are pre-trained based on a model with parameters that may not match the test subject. Evidence of the haptic feedback that the human operator is receiving can be seen in the middle plot, where the motor input is negative. This means that the controller essentially realized that the subject was not able to reach the desired position set by the human operator and produced negative torques on the robotic manipulator which the human operator would perceive as resistance.

In the final set of experiments, the use of FES as a haptic feedback was tested. In this experiment, the test subject was instructed to voluntarily move his leg similar to the ramp trial in the first set of experiments. The human operator would then observe the synchronized movements produced by the robotic manipulator. During the downward slope (e.g., leg is flexing), the human operator restricted the robot from moving past a certain position. The restricted robot's movement is mimicked by the subject's leg even though the subject is trying to flex his knee voluntarily. This robot and leg coordination can be explained as follows. The controller notices that the robotic manipulator is impeded from moving further, and thus increases the amount of electrical stimulation that results in the quadriceps contraction, which restricts the test subject from further moving downwards. The results from this experiment can be seen in Fig. 5. The instances when the human operator impedes the motion of the robot are indicated with an arrow in the top plots of Fig. 5. From the motor input plots, it can be observed where the human operator interferes, the input becomes negative which means the robot was trying to move in a direction that was against the human operator's intended direction. Also, the test subject indicated that he felt that the FES stimulation was more effectively resisting his knee from flexing when the human operator blocked the robot movement.

6 Discussion

The aim of this paper was to present a bilateral control scheme for an FES-based telerehabilitation system and validate it through experiments. With such as system, therapy sessions could be done from the leisure of the patient's own home to maintain muscle strength and help strengthen the neurological connection between the brain and motor neurons as a therapist physically oversees and interacts with them. The strength of this scheme is the incorporation of FES during telerehabilitation. Therapy sessions for patients with conditions like stroke involve not only increasing their joint's range of motion and muscle stretching exercises but also the need to strengthen weakened muscles. Systems that simply stretch or move a joint through a range of motion are providing only part of the needed therapy. Therefore, due to its physiological advantages, FES is an added benefit during telerehabilitation of persons with partial or complete loss of limb function [15]. Moreover, FES has neuroplastic effects as it helps to retrain active motor units and rebuild the weak connections between the brain and the motor neurons [13, 14].

The developed bilateral control scheme overcomes some of the challenges posed due to the use of FES in real-time control. The proposed nonlinear control scheme is proven to be stable despite uncertain and highly nonlinear musculoskeletal dynamics as well as unknown constant communication delays. However, it is important to note that the size of the communication delay has an effect on the gain tuning which affects the level of performance achieved. Another benefit of this controller is that the NN would adapt to the changes in the muscle model as patient's musculoskeletal dynamics change due to increases in muscle strength or any neuroplastic effects. The use of a second neural network in the controller helps avoid the requirement of the acceleration in the controller or the assumption of bounding the time derivative of the Ω function. The online adaptation of the NN is also beneficial due to evidence that has shown that after a person has an upper motor neuron injury the force-length/force-velocity relationship change due to spasticity [42,43]. The adaptiveness of the proposed scheme can potentially deal with changes in the dynamics due to spasticity. However, the controller's ability to adapt in these scenarios remains to be tested.

During rehabilitation sessions, patients usually differ in terms of the range of motion through which their limb can be moved. For example, a knee contracture in one patient can severely limit the range of motion. Therefore, one of the strengths of the proposed system is that a therapist has control over a patient's joint angle trajectories. This is extremely beneficial because therapy sessions can be customized to each patient and it can prevent injuries. In addition, the haptic feedback feature of the controller, which was highlighted in the third set of experiments, would provide evidence of observations to the therapist that he/she would use to alter the trajectories.

7 Conclusion

In this paper, we presented a controller that achieves position synchronization for an FES-based bilateral telerehabilitation system with mismatching unknown communication delays in the forward and backward channels. The proposed controller uses artificial neural networks, which were pre-trained offline, to compensate for the unstructured nonlinear musculoskeletal dynamics and adaptive based controllers for the structured nonlinear dynamics in the musculoskeletal and robotic systems. The Lyapunov stability analysis for the proposed controller was used to prove GUUB tracking performance. The controller was validated experimentally on an able-bodied male subject that shows its feasibility in a telerehabilitation set-up. Future experiments will be performed on subjects with stroke to show its clinical relevance.

Acknowledgments

This work was funded in part by the National Science Foundation award number 1511139.

References

1. Go AS, Mozaffarian D, Roger VL, Benjamin EJ, Berry JD, Blaha MJ, Dai S, Ford ES, Fox CS, Franco S, et al. Heart disease and stroke statistics-2014 update. Circulation. 2014; 129(3)
2. Mayo NE, Wood-Dauphinee S, Coöte R, Durcan L, Carlton J. Activity, participation, and quality of life 6 months poststroke. Arch. Phys. Med. Rehabil. 2002; 83(8):1035–1042. [PubMed: 12161823]
3. Kwakkel G, Kollen BJ, van der Grond J, Prevo AJ. Probability of regaining dexterity in the flaccid upper limb impact of severity of paresis and time since onset in acute stroke. Stroke. 2003; 34(9): 2181–2186. [PubMed: 12907818]
4. Durfee WK, Savard L, Weinstein S. Technical feasibility of teleassessments for rehabilitation. IEEE Trans. Neural Syst. Rehabil. Eng. 2007; 15(1):23–29. [PubMed: 17436872]
5. Zampolini M, Todeschini E, Guitart M, Hermens H, Ilsbroukx S, Macellari V, Magni R, Rogante M, Marchese S, Vollenbroek M, Giacomozzi C. Tele-rehabilitation: present and future. Ann Ist Super Sanita. 2008; 44:125–134. no. 0021-2571 (Linking). [PubMed: 18660562]
6. Huijgen BC, Vollenbroek-Hutten MM, Zampolini M, Opisso E, Bernabeu M, Van Nieuwenhoven J, Ilsbroukx S, Magni R, Giacomozzi C, Marcellari V, et al. Feasibility of a home-based telerehabilitation system compared to usual care: arm/hand function in patients with stroke, traumatic brain injury and multiple sclerosis. Journal of Telemedicine and Telecare. 2008; 14(5): 249–256. [PubMed: 18633000]
7. Gregory P, Alexander J, Satinsky J. Clinical telerehabilitation: applications for physiatrists. PM&R. 2011; 3(7):647–656. [PubMed: 21777864]
8. Kowalczewski J, Chong SL, Galea M, Prochazka A. In-home tele-rehabilitation improves tetraplegic hand function. Neurorehab. Neural. Re. 2011; 25(5):412–422.
9. Hermann VH, Herzog M, Jordan R, Hofherr M, Levine P, Page S. Telerehabilitation and electrical stimulation: An occupation-based, client-centered stroke intervention. The American Journal of Occupational Therapy. 2010; 64(1):73–81. [PubMed: 20131566]
10. Reinkensmeyer DJ, Pang CT, Nessler JA, Painter CC. Web-based telerehabilitation for the upper extremity after stroke. IEEE Trans. Neural Syst. Rehabil. Eng. 2002; 10(2):102–108. [PubMed: 12236447]
11. Popescu VG, Burdea GC, Bouzit M, Hentz VR. A virtual-reality-based telerehabilitation system with force feedback. IEEE Trans. Inf. Technol. Biomed. 2000; 4(1):45–51. [PubMed: 10761773]
12. Simonsen, D., Irani, R., Nasrollahi, K., Hansen, J., Spaich, EG., Moeslund, TB., Andersen, OK. Replace, Repair, Restore, Relieve–Bridging Clinical and Engineering Solutions in Neurorehabilitation. Springer; 2014. Validation and test of a closed-loop tele-rehabilitation system

based on functional electrical stimulation and computer vision for analysing facial expressions in stroke patients; p. 741-750.

13. Nagai, MK., Marquez-Chin, C., Popovic, MR. Translational Neuroscience. Springer; 2016. Why is functional electrical stimulation therapy capable of restoring motor function following severe injury to the central nervous system?; p. 479-498.
14. Popovic, MR., Masani, K., Micera, S. Functional Electrical Stimulation Therapy: Recovery of Function Following Spinal Cord Injury and Stroke. London: Springer London; 2012. p. 105-121.
15. Peckham PH, Knutson JS. Functional electrical stimulation for neuromuscular applications. Annu. Rev. Biomed. Eng. 2005; 7:327–360. [PubMed: 16004574]
16. Carignan C, Krebs H. Telerehabilitation robotics: bright lights, big future? Journal of Rehabilitation Research & Development. 2006; 43:695–710. [PubMed: 17123209]
17. Sharma N, Stegath K, Gregory CM, Dixon WE. Nonlinear neuromuscular electrical stimulation tracking control of a human limb. IEEE Trans. Neural Syst. Rehabil. Eng. 2009; 17(6):576–584. [PubMed: 19497828]
18. Sharma, N., Patre, P., Gregory, C., Dixon, W. Proceedings of ASME Dynamic Systems and Control Conference. ASME; 2009. Nonlinear control of NMES: Incorporating fatigue and calcium dynamics.
19. Sharma N, Gregory C, Dixon WE. Predictor-based compensation for electromechanical delay during neuromuscular electrical stimulation. IEEE Trans. Neural Syst. Rehabil. Eng. 2011; 19(6): 601–611. [PubMed: 21968792]
20. Sharma N, Gregory CM, Johnson M, Dixon WE. Closed-loop neural network-based NMES control for human limb tracking. IEEE Trans. Control Syst. Technol. 2012; 20(3):712–725.
21. Ajoudani A, Erfanian A. A neuro-sliding-mode control with adaptive modeling of uncertainty for control of movement in paralyzed limbs using functional electrical stimulation. Biomedical Engineering, IEEE Transactions on. 2009; 56(7):1771–1780.
22. Alibeji N, Kirsch N, Farrokhi S, Sharma N. Further results on predictor-based control of neuromuscular electrical stimulation. IEEE Trans. Neural Syst. Rehabil. Eng. 2015
23. Jezernik S, Wassink RG, Keller T. Sliding mode closed-loop control of FES controlling the shank movement. IEEE Trans. Biomed. Eng. 2004; 51(2):263–272. [PubMed: 14765699]
24. Cheng T, Wang Q, Kamalapurkar R, Dinh H, Bellman M, Dixon W. Identification-based closed-loop NMES limb tracking with amplitude-modulated control input. IEEE Trans. Cybern. 2015 (Accepted).
25. Chopra N, Spong M, Ortega R, Barabanov N. On position tracking in bilateral teleoperation. Proceedings of the 2004 American Control Conference. 2004; 6:5244–5249.
26. Chopra N, Spong M, Ortega R, Barabanov N. On tracking performance in bilateral teleoperation. IEEE Transactions on Robotics. 2006; 22(4):861–866.
27. Chopra N, Spong M, Lozano R. Synchronization of bilateral teleoperators with time delay. Automatica. 2008; 44(8):2142–2148.
28. Chopra N, Berestesky P, Spong M. Bilateral teleoperation over unreliable communication networks. IEEE Transactions on Control Systems Technology. 2008; 16(2):304–313.
29. Kitamura, T., Sakaino, S., Tsuji, T. IECON 2015-41st Annual Conference of the IEEE Industrial Electronics Society. IEEE; 2015. Bilateral control using functional electrical stimulation; p. 002 336-002 341.
30. Alibeji, NA., Kirsch, NA., Sethi, A., Sharma, N. ASME 2014 Dynamic Systems and Control Conference. American Society of Mechanical Engineers; 2014. A state synchronization controller for functional electrical stimulation-based telerehabilitation; p. V003T43A004-V003T43A004.
31. Alibeji, N., Kirsch, N., Sharma, N. Control of functional electrical stimulation in the presence of electromechanical and communication delays; 6th International IEEE/EMBS Conference on NER; 2013. p. 299-302.
32. Sharma N. A predictor-based compensation for electromechanical delay during neuromuscular electrical stimulation-II. Proc. of ACC. 2012:5604–5609.
33. Sharma N, Bhasin S, Wang Q, Dixon WE. Predictor-based control for an uncertain euler-lagrange system with input delay. Automatica. 2011; 47(11):2332–2342.

34. Schauer T, Negard NO, Previdi F, Hunt KJ, Fraser MH, Ferchland E, Raisch J. Online identification and nonlinear control of the electrically stimulated quadriceps muscle. Control Eng. Pract. 2005; 13:1207–1219.

35. Li, Z., Xia, Y., Su, C-Y. Intelligent Networked Teleoperation Control. Springer; 2015.

36. Winter, D. Biomechanics and motor control of human movement. Wiley; 2009.

37. Chen M, Ge SS, How BVE. Robust adaptive neural network control for a class of uncertain mimo nonlinear systems with input nonlinearities. IEEE Transactions on Neural Networks. 2010; 21(5): 796–812. [PubMed: 20236884]

38. Lewis, FL., Dawson, DM., Abdallah, CT. Robot manipulator control: theory and practice. CRC Press; 2003.

39. Dixon, WE., Behal, A., Dawson, DM., Nagarkatti, S. Nonlinear Control of Engineering Systems: A Lyapunov-Based Approach. Birkhäuser Boston; 2003.

40. Khalil, H. Nonlinear Systems. 3rd. Prentice Hall; 2002.

41. Popović D, Stein R, Oğuztöreli M, Lebiedowska M, Jonić S. Optimal control of walking with functional electrical stimulation: a computer simulation study. IEEE Trans. Rehabil. Eng. 1999; 7(1):69–79. [PubMed: 10188609]

42. Gao F, Zhang L-Q. Altered contractile properties of the gastrocnemius muscle poststroke. Journal of Applied Physiology. 2008; 105(6):1802–1808. [PubMed: 18948443]

43. Gray V, Rice CL, Garland SJ. Factors that influence muscle weakness following stroke and their clinical implications: a critical review. Physiotherapy Canada. 2012; 64(4):415–426. [PubMed: 23997398]

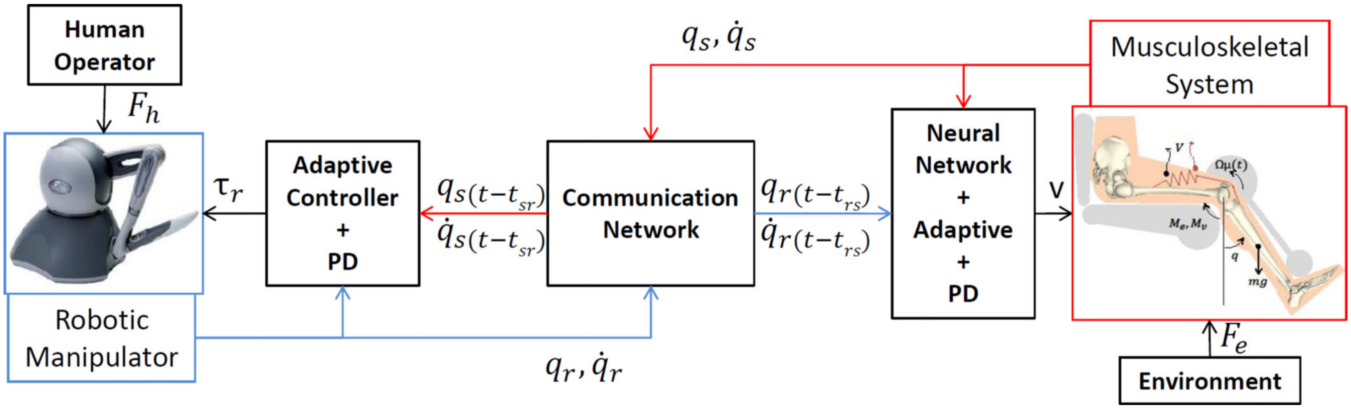

Fig. 1.

The control scheme uses an adaptive and PD control for the robotic manipulator, and a combination of neural networks, adaptive, and PD control for the musculoskeletal system. The communication network introduces a delay in any signal that passes through it which can be different passing from the robot side to the subject side and vice-versa.

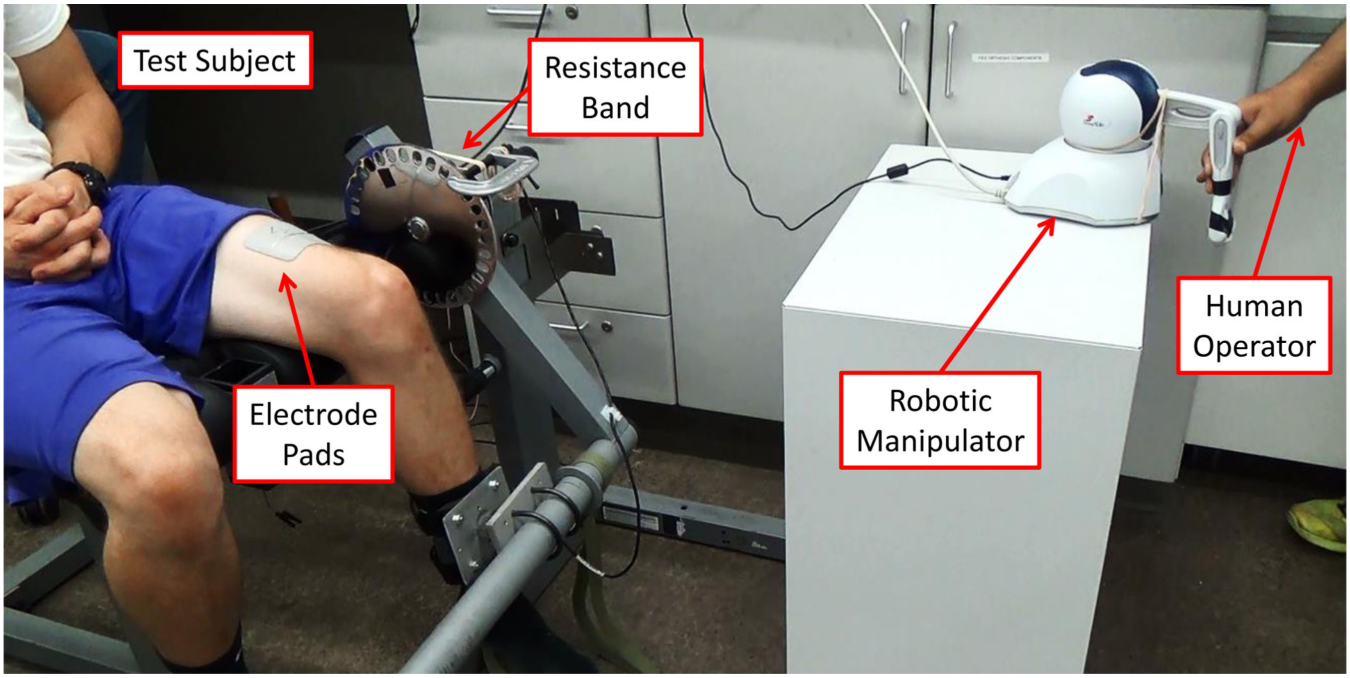

Fig. 2.

The testbed used for the preliminary experiments consists of a leg extension machine modified with a optical encoder and resistance bands for the test subject. A Phantom Omni is used as a robotic manipulator for which the human operator to interact with. The communication network and delays are implemented virtually in the software.

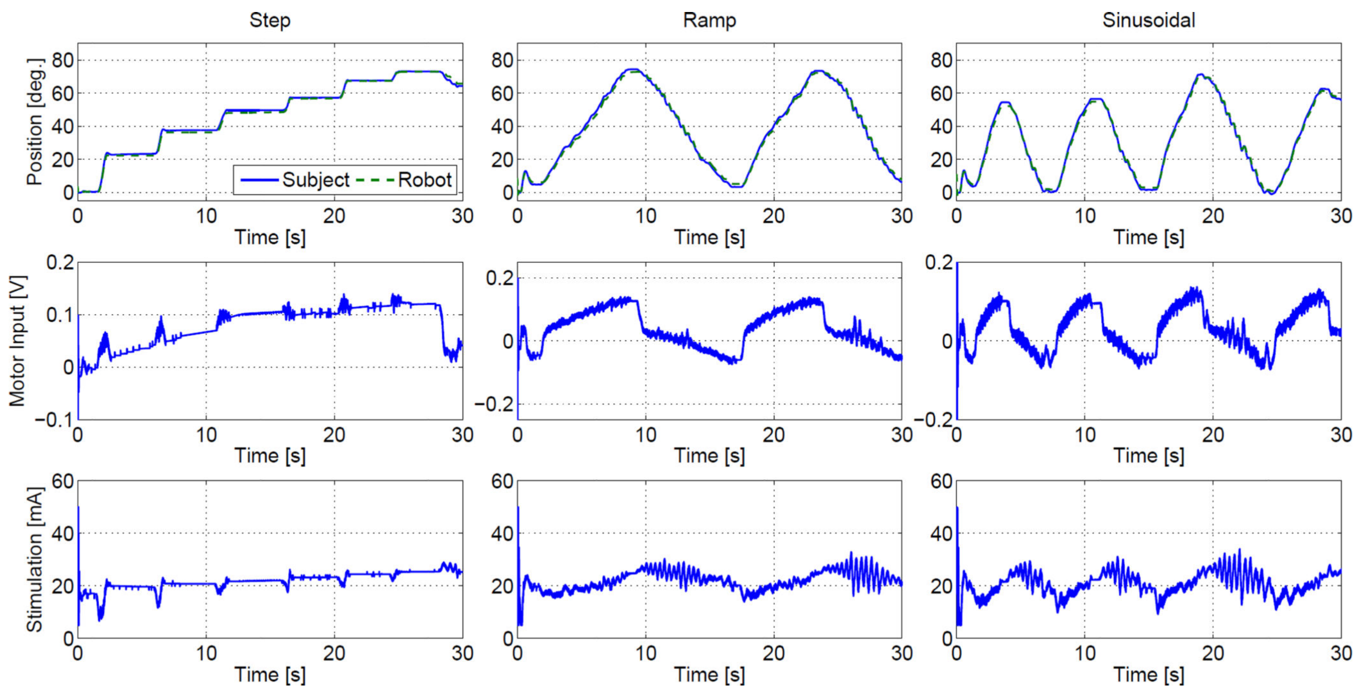

Fig. 3.

The control performance in the case where the test subject is driving the system for the three trials. The top plots show the position of the delayed subject's knee angle and the robot's link angle, i.e., q_r and $q_{s\tau_r}$. The input to the motor and FES system during these trials are shown in the middle and bottom plots, respectively.

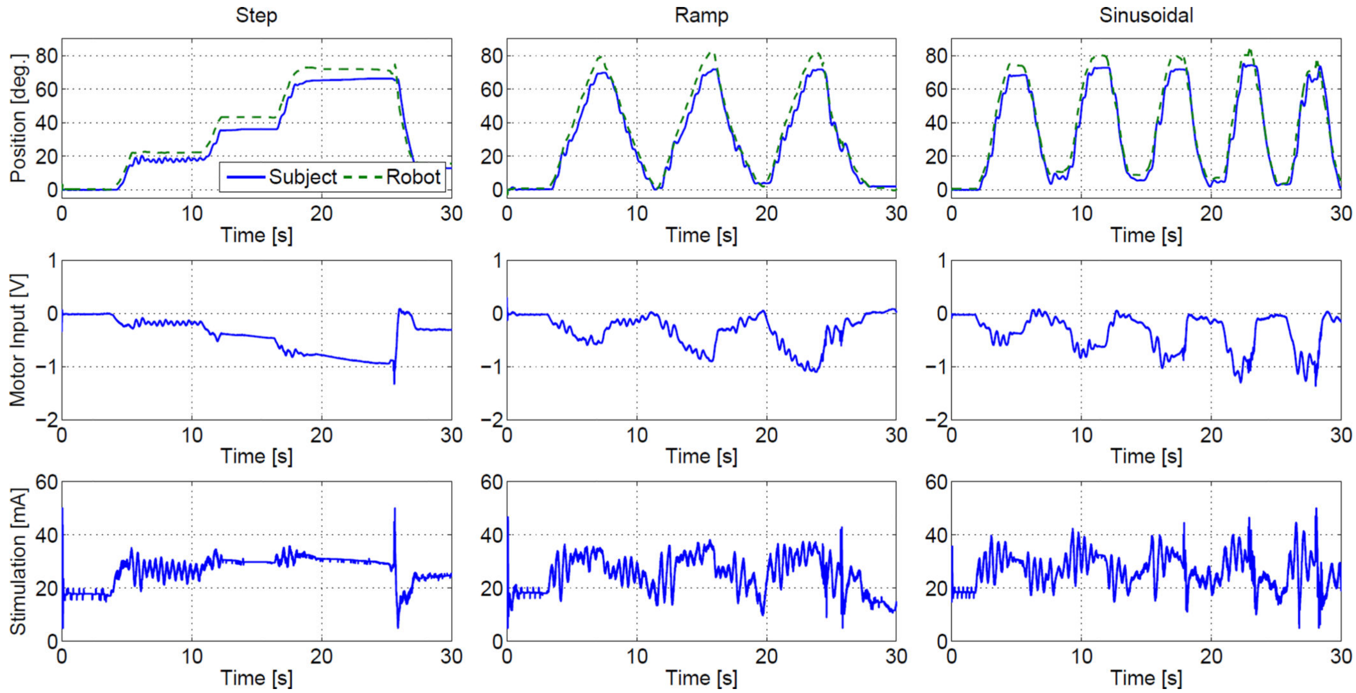

Fig. 4.

The control performance in the case where the human operator is driving the system for the three trials. The top plots show the position of the subject knee angle and delayed robot link angle, i.e., q_s and $q_{r\tau_s}$. The input to the motor and FES system during these trials are in the middle and bottom plots, respectively.

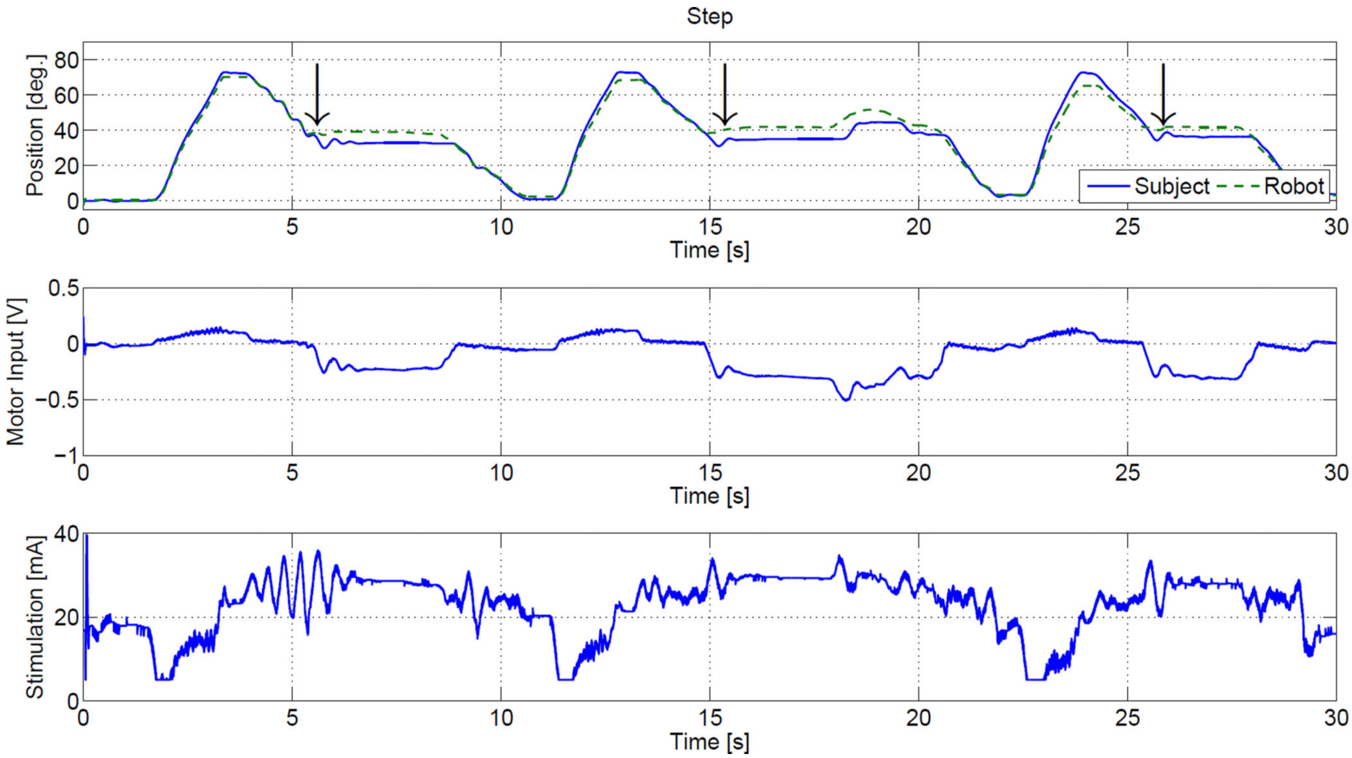

Fig. 5.

The control performance in the case where the test subject is driving the system but the human operator impedes the movement of the robotic manipulator resulting in FES-based haptics feedback. The top plots show the subjects knee angle and delayed robot link angle and an arrow indicates when the human operator impedes the robot. The input to the motor and FES system during these trials are in the middle and bottom plots, respectively.